RSC Advances

ROYAL SOCIETY OF CHEMISTRY

www.rsc.org/advances

Synthesis, crystal structures, magnetic properties and DFT calculations of nitrate and oxalate complexes with 3,5 dimethyl-1-(2´-pyridyl)-pyrazole-Cu(II)

Pampi Pal,[†] Saugata Konar*[,‡], Mohamed Salah El Fallah[#], Kinsuk Das*[,||], Antonio Bauzá[⊥], Antonio Frontera*[,⊥] and Subrata Mukhopadhyay[‡]

[†] *Assistant Teacher in Chemistry, Ghoshpara Nischinda Balika Vidyapith, Bally, Howrah 711227, India*

[‡] *Department of Chemistry, Jadavpur University, Jadavpur, Kolkata 700032, India. Email: saugata.konar@gmail.com*

[#] *Departament de Química Inorganica, Universitat de Barcelona, Marti I Franques, 1-11 08028 Barcelona, Catalunya, Spain*

[||] *Department of Chemistry, Darjeeling Government College, Darjeeling 734101, India. Email: kdaschem@yahoo.in*

[⊥] *Departament de Química, Universitat de les Illes Balears, Crta. de Valldemossa km 7.5, 07122 Palma (Baleares), Spain. E-mail: toni.frontera@uib.es*

Abstract

The synthesis, crystal structures and magnetic property of an uncommon oxalate-containing copper(II) chain of formula $[Cu(L)(Ox)_2(H_2O)]_n$ (**2**), where L = 3,5 dimethyl-1-(2´-pyridyl)-pyrazole and a mononuclear Cu(II) complex $[Cu(L)(NO_3)_2]$ (**1**) derived from the same ligand, which can be used as the precursor of compound **2** are reported. The structure of **2** consists of tridentate oxalate-bridged ($\mu_{1,2,3}$) copper(II) chains, ligand (L) and crystallization water molecules. Variable-temperature magnetic susceptibility measurements of **2** show the occurrence of a weak ferromagnetic interaction through the oxalate bridge [$J = +1.95 \pm 0.08$ cm^{-1}]. The small J value can be interpreted as a consequence of the almost nil overlap between the Cu(II) ions through the bridging ligand due to the different character (axial and equatorial), giving quasi-orthogonal magnetic orbitals. DFT calculations have been used to rationalize several aspects including the magnetic coupling mechanism and the interesting noncovalent interactions observed in the solid state architecture of compounds **1** and **2**.

Keywords: X-ray crystal structure; Tridentate $\mu_{1,2,3}$ oxalate bridging; Ferromagnetism; DFT calculations; Noncovalent interactions

Introduction

Inorganic chemists have shown interest in synthesizing coordination complexes of heterocyclic base ligands because of their broad applicability in catalysis, in designing molecular ferromagnets, in biological modeling as liquid crystals and as heterogeneous catalysts.[1,2] It is well known that the careful selection of the organic ligands is one of the key factors for the synthesis of the coordination compounds with novel structures.

Oxalate ion has been demonstrated to be excellent connector for the construction of organic–inorganic hybrid polymeric compounds. The oxalate group (dianion of the ethanedioic acid, H_2Ox) is a classical ligand in coordination chemistry and in magneto-structural studies due to the great number of coordination modes that it exhibits in its metal complexes[3–6] together with its remarkable ability to mediate strong magnetic interactions between the paramagnetic metal ions when acting as a bis-bidentate bridge, the metal-metal separation being larger than 5.4 Å.[6] In the available oxalate copper(II) complexes, the $\mu_{1,2,3,4}$-bis-chelating mode is more frequently exhibited, while the number of structurally characterized complexes in which the oxalate group acts as tridentate ligand is scarce[7] that exhibit weak antiferromagnetic interactions between copper(II) ions.[8–13] The ferromagnetic complexes with tridentate coordination mode are very rarely reported. Here, we report a weak ferromagnetic tridentate oxalato bridged 1D Cu(II) polymeric complex along with a monomeric Cu(II) complexes derived from strongly coordinating bidentate pyridyl-pyrazole (L) ligand. Magnetic susceptibility measurements reveal a weak ferromagnetic interaction between the adjacent Cu(II) ions separated by 5.399 Å. There are several oxalato bridged Cu(II) complexes among which some are antiferromagnetic in nature and some other shows ferromagnetic behaviour (*vide infra*). Keeping all these results in mind we extend our work beyond the monomeric Cu(II) complex (complex **1**) derived from pyridyl-pyrazole (L) ligand and finally have synthesized a weak ferromagnetic tridentate oxalato bridged 1D Cu(II) polymeric complex (complex **2**) from the same ligand in two different ways (Scheme 1). The first one was synthesized by 1:1 condensation between $K_2[Cu(Ox)_2]$ and the ligand 'L' in methanol solvent and the second one was synthesized from the condensation of the complex **1** with oxalic acid in aqueous media. Even though a great variety of oxalato-bridged polynuclear complexes have been structurally and magnetically characterized (from discrete dimers to three-dimensional systems), to the best of our knowledge only a few weak ferromagnetically one-dimensional $\mu_{1,2,3}$ tridentate oxalato-bridged copper(II) compounds are known.[14] Moreover, compound **2** is the first example of a the tridentate oxalate-bridged ($\mu_{1,2,3}$) copper(II) based on pyridyl pyrazole ligand. Finally, we also report herein density functional theory (DFT) calculations where we analyze two interesting aspects of the complexes. First, we study the interesting π-hole noncovalent interactions involving the coordinated nitro ligands in compound **1**. As a matter of fact, the importance of this particular interaction in supramolecular chemistry has been recently investigated[15] combining a comprehensive analysis of the CSD and theoretical calculations. Second, the magnetic properties of compound **2** have been rationalized using the broken-symmetry approach and analyzing the spin density of a Cu_2 dimeric model of the polymeric chain.

Experimental section

Materials

All chemicals were of reagent grade, purchased from commercial sources and used without further purification. 2-chloro pyridine, acetyl acetone and hydrazine hydrate (Aldrich) were used without further purification.

Physical Measurements

Elemental analyses (C, H and N) of the ligand and the metal complexes were determined with a Perkin–Elmer CHN analyzer 2400. Magnetic susceptibilities were measured on a Quantum Design MPMSXL5 (SQUID) magnetometer. Diamagnetic corrections were estimated from Pascal's constants for all constituent atoms. The electronic spectra of the complexes in methanol solution were recorded on a Hitachi model U-3501 spectrophotometer. FT–IR spectra were recorded on a Perkin Elmer; model RX–1(KBr disk, 4000–400 cm^{-1}) spectrometer.

Synthesis of 3,5 dimethyl-1-(2´-pyridyl) pyrazole (L)

The ligand L (3, 5 dimethyl-1-(2´-pyridyl) pyrazole) was synthesized following the reported method.[16]

Synthesis of Compound $[Cu(L)(NO_3)_2]$ (1)

A methanolic solution (10 mL) of the ligand L (0.173g, 1 mmol) was added drop wise to a solution of $Cu(NO_3)_2$, $6H_2O$ (0.295g, 1 mmol) in the same solvent (10 mL) with constant stirring which continued for 2 h. The separated resulting green compound was filtered and dried over silica gel in desiccators. Then the solution was left for slow evaporation. After one week deep green X-ray quality crystals of **1** were isolated. (Yield: 62%). Anal. Calc. for $C_{10}H_{11}CuN_5O_6$: C,33.26; H,3.05; N,19.40. Found: C,33.21; H,3.01; N,19.42. μ_{eff} (at 298K) = 1.72 B.M. $\lambda_{max/nm}$ = 287 and 327 (Fig. S1). Main FT-IR absorptions, (KBr pellets): ν = 1429 (s), 1315 (s), 1051 (m) (Fig. S2).

Synthesis of Compound $[Cu(L)(Ox)_2(H_2O)]_n$ (2)

The methanolic solution of $K_2[Cu(Ox)_2]\cdot 2H_2O$ (0.354 g, 1 mmol) was added to an aqueous methanolic solution of the ligand L (0.173 g, 1 mmol). The mixture was stirred for 2 h, filtered and kept for slow evaporation. After one week blue X-ray quality crystals of **2** were obtained. (Yield: 69.5%). Anal. Calc. for $C_{24}H_{24}Cu_2N_6O_9$: C,43.14; H,3.59; N,12.58. Found: C,43.11; H,3.57; N,12.60. $\lambda_{max/nm}$ = 291 and 318 (Fig. S3). FT-IR absorptions, (KBr pellets): ν = 1640 (s), 1484 (m), 1341 (s), 1059 (m), 795 (s) (Fig. S4).

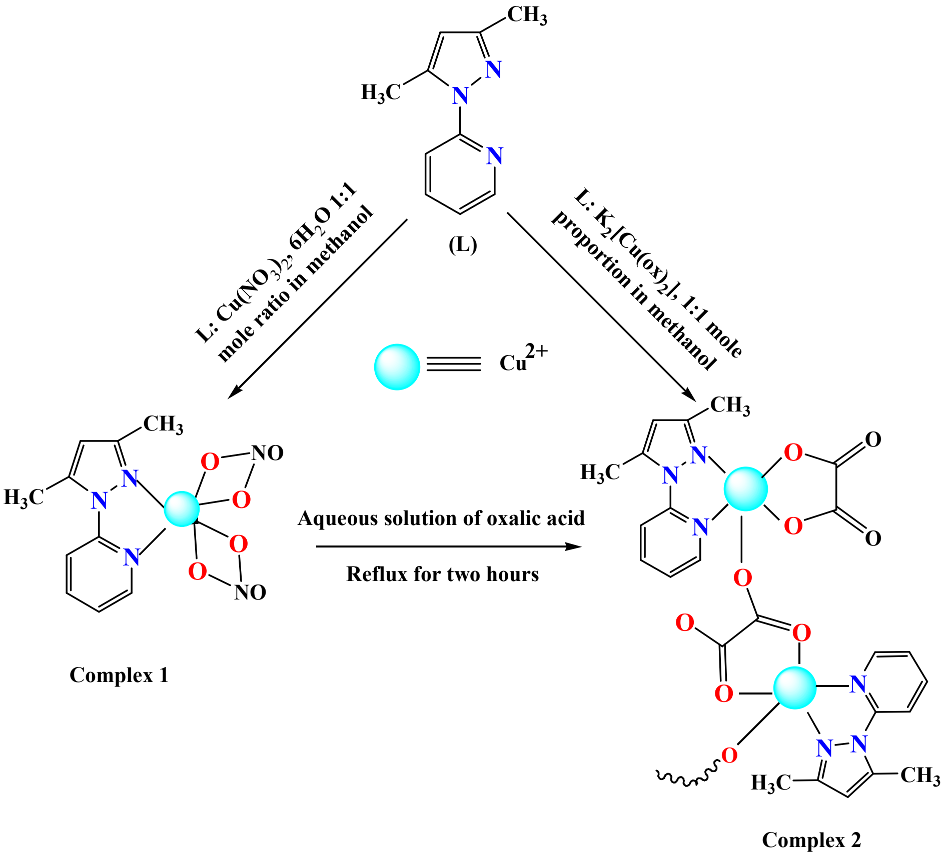

Scheme 1

X-ray crystallographic data collection and refinement

Selected crystal data for **1** and **2** are given in Table S1 and selected metrical parameters of the complexes are given in Table S2. For both complexes **1** and **2** data collections were made using Bruker SMART APEX II CCD area detector equipped with graphite monochromated Cu and Mo Kα radiation (λ = 0.71073 Å) source in φ and ω scan mode at 90(2) and 150(2) K respectively. Cell parameters refinement and data reduction were carried out using the Bruker SMART and Bruker SAINT softwares[17] for all the complexes. The structure of all the complexes were solved by conventional direct methods and refined by full-matrix least square methods using F^2 data. SHELXS-97 and SHELXL-97 programs[18] were used for structure of all the complexes solution and refinement respectively. For both complexes non hydrogen atoms were refined anisotropically till the convergence is attained.

Theoretical methods

The energies of all complexes included in this study were computed at the BP86-D3/def2-TZVP level of theory. We have used the crystallographic coordinates for the theoretical analysis of the non-covalent interactions observed in the solid state. This level of theory has been shown useful and reliable to study noncovalent interactions like those analyzed herein.[19a,b] The calculations have been performed by using the program TURBOMOLE version 6.5.[20] For the calculations we have used the BP86 functional with the latest available correction for dispersion (D3).[21] The Bader's "Atoms in molecules" theory has been used to study the interactions discussed herein by means of the AIM all calculation package.[22]

The magnetic coupling constants are described using the Heisenberg model. The hybrid B3LYP functional[23a-c] has been used in all calculations as implemented in Gaussian-09,[24] using the 6-31+G* basis set for all atoms. The approach used to determine the exchange coupling constants for dinuclear and trinuclear complexes has been described before in the literature.[25a-d]

Results and discussion

Crystal Structure Description of Complex 1

The perspective view of molecular structure of complex **1** with atom numbering scheme is shown in Fig. 1. Complex **1** crystallizes in space group P-1 in which the unit cell is comprised of two molecules.

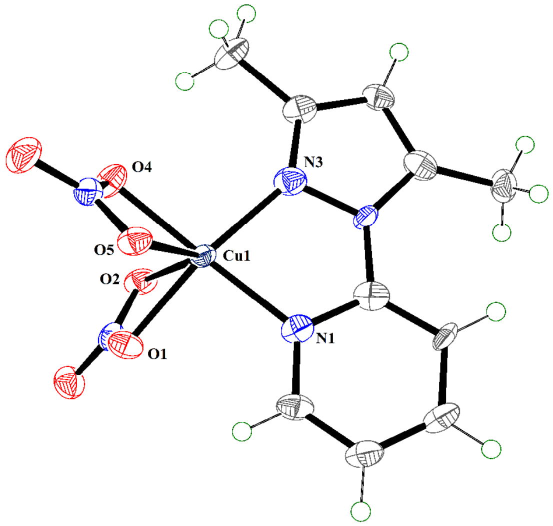

Fig. 1 Molecular structure of complex **1** with ellipsoids drawn at 50% probability. Color code: Cu(II), sky; O, red; N, blue; C, grey; H, light green.

Complex **1** is distorted octahedral where the ligand L, spans the adjacent positions [N1–Cu1–N3=81.54(6)°] as a neutral bidentate NN donor *via* one pyridyl nitrogen (N3) and one pyrazolyl nitrogen (N1). The other four positions of the octahedral geometry are occupied by two oxygen atoms from two different bidentate nitrate anions (O1, O2 and O4, O5). The Cu – N bond distances [Cu1–N1=1.947(18) Ǻ, Cu1–N3=1.977(17) Ǻ] and the copper-oxygen bond lengths [Cu1–O1=2.419(16) Ǻ, Cu1–O2=1.972(16) Ǻ, Cu1–O4=2.481(16) Ǻ and Cu1–O5=1.991(16) Ǻ] are in accord with those values reported previously for similar type of six coordinated octahedral Cu(II) complexes.[26–28] Cu(II) atom sits in the same mean plane constituted by N1N3O5O2 atoms. The three *trans* angles are N1-Cu1-O5 (160.05°), N3-Cu1-O2 (163.47°) and O4-Cu1-O1 (128.69°) departed from the ideal trans angle of 180° due to some steric obligations. This is most likely due to the small bite angles [O1–Cu1–O2=58.05(5)° and O4–Cu1–O5=56.74(5)°] of the bidentate nitrate ligand, which may induce a distortion in the geometry of the complex.[29] In this coordination game the pyridyl part is slightly twisted by 9.25° with respect to the pyrazole part. There are two types of anion–π interactions involving the non coordinating atoms O(6) and O(3) of the nitrate anions that are orientated towards the π-face (Fig. 2) of the ligand, pointing to the middle of the N2–C4 bond (the anion–π distances are summarized in Table 1). It is remarkably the short distance observed for the N(5)-O(6)···π contact (< 3.0 Å) that is indicative of a strong interaction. As demonstrated below in the theoretical study by molecular electrostatic potential (MEP) calculations this part of the π-system is the most adequate for interacting with electron rich moieties.

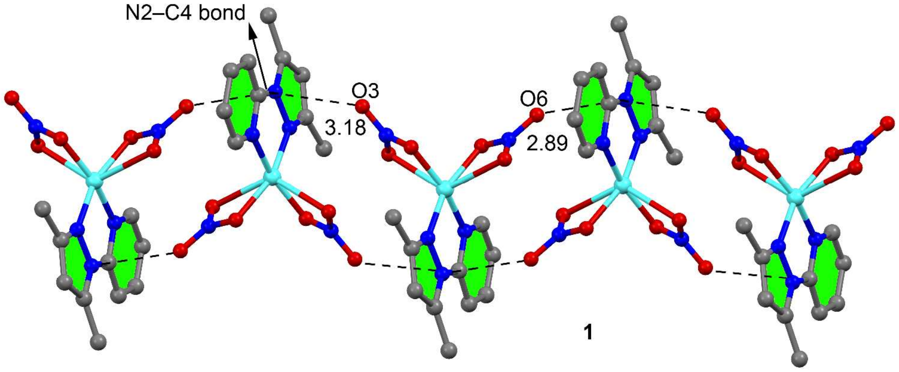

Fig. 2 Anion–π interaction along *a* axis in **1** to form an infinite 1D chain. Distances to the N–C ring centroid are given in Å. Hydrogen atoms are omitted for clarity. Color code: Cu(II), sky; O, red; N, blue; C, grey.

Table 1 Geometric features (distances in Å and angles in degrees) of the anion–π interactions observed in complex **1** (Cg = centre of gravity C4–N2 bond)

Interaction	O···N	O···C	∠N–O···Cg	∠O···Cg–N
N(4)-O(3)···π	3.128(5)	3.387(6)	132.8	79.1
N(5)-O(6)···π	2.964(5)	2.974(7)	134.4	89.6

Structural description of complex 2

The Perspective view of complex **2** with atom numbering schemes is shown in Fig. 3. The complex crystallizes in space group C2/c. The crystal structure of title compound reveals the presence of water molecule of crystallization with the neutral [Cu(Ox)(L)] moiety. The unit cell of **2** comprises of four molecules. The complex units are stacked in parallel and linked one to other through long Cu-O distances forming a one dimensional chain along the crystallographic '*a*' axis (Fig. S5). As indicated in the structural part of **2** two oxygen atoms of one bridging oxalate anions (O2 and O4), one oxygen of other bridging oxalate anion (O1) and two cis-coordinated nitrogen atoms [one from pyrazole (N3) and other from pyridine (N1)] of the ligand constitute a slightly distorted tetragonal square pyramid surrounding the

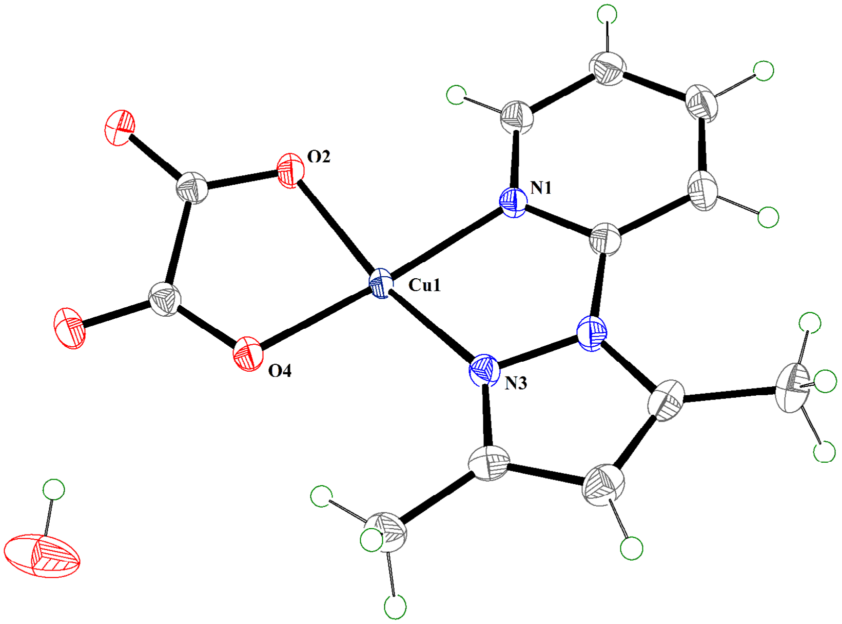

Fig. 3 Molecular structure of complex **2** with ellipsoids drawn at 50% probability. Color code: Cu(II), sky; O, red; N, blue; C, grey; H, light green.

Cu(II) ion. Two copper atoms are crystallographically indistinguisible. The equatorial Cu – O_{basal} [Cu1-O2 (1.951Å) and Cu1-O4 (1.924Å)] and Cu–N [Cu1-N1 (1.988Å) and Cu1-N3 (1.988Å)] bond distances are comparatively shorter than Cu–O_{axial} bond distance (Cu1–O1 = 2.284Å). The lengthening of the axial bond distance can be explained by the fact that the informing the axial bond less s- character has been utilized. In this situation the unpaired electron resides in a $d_{x^2-y^2}$ type orbital pointing to the four atoms with short metal–ligand distances (in the basal plane). The overlapping density between σ type orbitals should be rather small, while the 2p orbitals of the bridging axial oxygen (O1) atom, which is involved in the axial interaction, is approximately orthogonal to the $d_{x^2-y^2}$ orbital of the Cu(II) ion. Cu atom is displaced by 0.226Å from the N_2O_2 least square plane (N1O2O4N3) towards the axial O1 atom. The angles around the copper atom in it are close to ideal angle 90°. The metal-metal separation (Cu–Cu) within the chain of stacked molecules is 5.393Å. These values are more or less similar to the intramolecular Cu–Cu distance (5.399Å) in the asymmetrical binuclear cation [(dien)Cu(μ-ox)Cu(H_2O)$_2$-(tmen)]$_2$ (dien = diethylenetriamine and tmen = NNN′N′-tetramethylenediamine),[30] but are somewhat longer than the value of 5.29 Å, reported for the sheet like polymer [$Cu_2(ox)_2(pyz)_3$]$_n$ (pyz = pyrazine).[31] Pyrazole part is slightly twisted by an angle 2.31° with respect to the pyridyl ring. The oxalate and pyridyl part is twisted by an angle 17.03° whereas the same with pyrazole part is 17.8°.

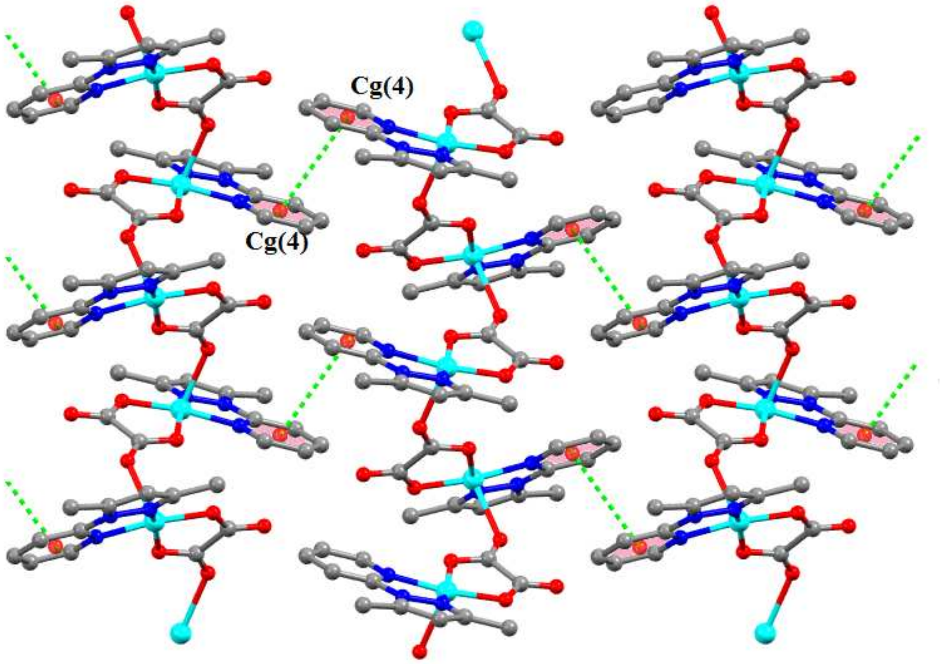

Fig. 4 π–π interaction along *c* axis in **2** to form 2D sheet. Hydrogen atoms are omitted for clarity. Color code: Cu(II), sky; O, red; N, blue; C, grey.

A two-dimensional supramolecular sheet (Fig. 4) is formed in complex **2** by multiple face-to-face π–π stacking interactions between the 1D infinite chains that involve the pyridine rings [Cg(4)], N1-C1-C2-C3-C4-C5] of one chain with the symmetry related (1-X,-Y,1-Z) pyridine rings [Cg(4)] of the neighboring chain (Table 2). Each molecule of [Cu(L)(Ox)] is assembled by C–H/π interactions along *c*-axis (Fig. 5) involving the one C(methyl)–H group, C(10)–H(10B) donor group of pyrazole ring and another pyridine ring Cg(4) [the ring centroid defined by N1-C1-C2-C3-C4-C5 atoms] of symmetry 3/2-X,1/2-Y,1-Z and another type involving C(10)–H(10C) donor group of pyrazole ring and aromatic pyrazole ring Cg(3) (the ring centroid defined by N2-N3-C6-C7-C8 atoms) of symmetry 3/2-X,-1/2-Y,1-Z (Fig. 5) (Table 3).

Table 2 Geometric features (distances in Å and angles in degrees) of the π–π interactions obtained for **2**

Cg(Ring I)–Cg(Ring J)	Cg–Cg	Cg(I)•••Perp	Cg(J)•••Perp	Α	Β	Γ	Symmetry
Cg(4)–Cg(4)	3.731(3)	3.372	3.372	0.02	25.34	25.34	1-X,-Y,1-Z

α = Dihedral angle between ring I and ring J (°); β= Cg(I)-->Cg(J) or Cg(I)-->Me vector and normal to plane I (°); γ = Cg(I)-->Cg(J) vector and normal to plane J (°);Cg-Cg = Distance between ring Centroids (Å); CgI----Perp = Perpendicular distance of Cg(I) on ring J (Å); CgJ----Perp = Perpendicular distance of Cg(J) on ring I (Å); Cg(4) = centre of gravity of ring [N1-C1-C2-C3-C4-C5] for complex **2**.

Table 3 Geometric features (distances in Å and angles in degrees) of the C–H/π interactions obtained for **2**

C–H···Cg(Ring)	H···Cg (Å)	C–H···Cg (°)	C···Cg (Å)	Symmetry
C10 – H10B···Cg(4)	2.82	165	3.752(4)	3/2-X,1/2-Y,1-Z
C10 – H10C···Cg(3)	2.60	138	3.368(3)	3/2-X,-1/2-Y,1-Z

For complex **2**, Cg(4) = centre of gravity of ring [N1-C1-C2-C3-C4-C5], Cg(3) = centre of gravity of ring [N2-N3-C6-C7-C8].

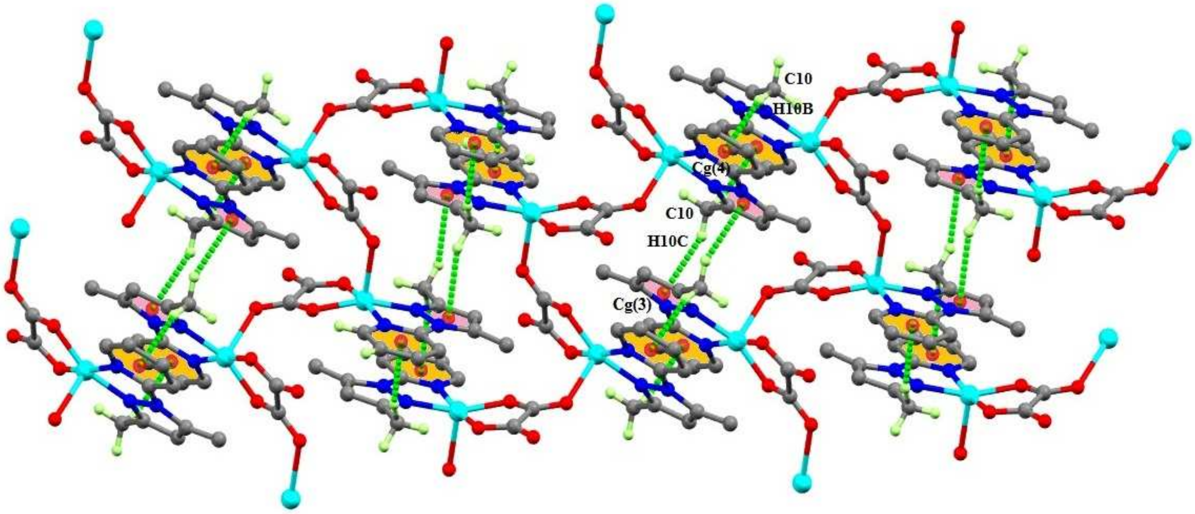

Fig. 5 C-H/π along *a* axis to form 2D sheet in **2**. Non related hydrogen atoms are omitted for clarity. Color code: Cu(II), sky; O, red; N, blue; C, grey; H, light green.

Magnetic Properties

The magnetic property of complex **2** is shown in Fig. 6 as $\chi_M T$ vs. T and $M/N\mu_B$ vs. H (inset) respectively. The values of $\chi_M T$ at 300 K are 0.5 $cm^3mol^{-1}K$ which is as expected for magnetically quasi-isolated spin doublets (g > 2.00). Starting from the room temperature $\chi_M T$ values remain practically constant up to 50 K and below 50 K it increase quickly to 1.1 $cm^3mol^{-1}K$ at 2 K. This global feature is characteristic of very weak ferromagnetic interactions. The $M/N\mu_B$ value at 5 T is close to 1.1 and the curve practically follows the Brillouin law, assuming g > 2.0, logical for any Cu(II) ion. Complex **2** is, actually, a one-dimensional system in which the copper atoms are linked by oxalato bridging ligands in axial-equatorial form. This feature gives a uniform S = ½ system (with J = coupling parameter for the Cu-bridge-Cu pathway). The fit of the magnetic data has been carried out using the formula given by Kahn for this kind of uniform ferromagnetic S = ½ chains[32]. According to Kahn's model[6,32], the coupling constant 'J' can be decomposed into two terms, one positive (ferromagnetic, J_F) and the other negative (antiferromagnetic, J_{AF}), the expression being $J = J_F + J_{AF}$. In such a model, the value of the negative term is proportional to the square of the overlap integral (S^2) between the two metal centered magnetic orbitals. In the case of complex **2**, the poor overlap between the two parallel magnetic orbitals through the two OCO oxalate set of atoms would lead to a weak ferro- or antiferromagnetic coupling.

The best-fit parameters obtained with this model are $J = +1.95 \pm 0.08$ cm^{-1}, $g = 2.21 \pm 0.01$ and $R = 1.1 \times 10^{-4}$. This result is a signature of the very weak ferromagnetic coupling mediated through the bridging ligands. The small J value can be interpreted as a consequence of the almost nil overlap between the Cu(II) ions through the ligand due to the different character (axial and equatorial), giving quasi-orthogonal magnetic orbitals. The symmetry of the Cu(II) ion is distorted square-pyramidal (τ parameter = 0.18; 0 for square pyramidal and **1** for trigonal bipyramidal). The major tendency to adopt the square pyramidal geometry avoids the necessary molecular overlap because the electronic density in a square pyramidal is in the d_{x2-y2} orbital. No important density is in the d_{z2} orbital (which corresponds to axial direction). The calculated J value must be taken with care, because being so small, any interchain coupling will be of the similar order of magnitude (but antiferromagnetic).

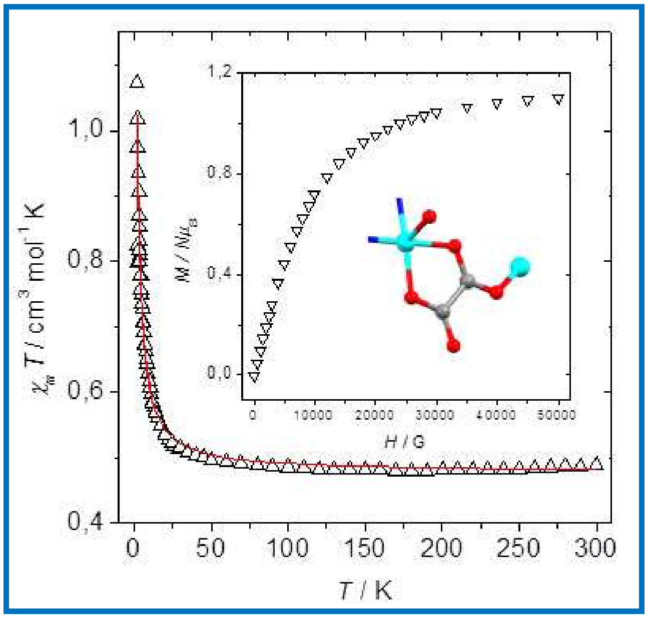

Fig. 6 $\chi_M T$ vs. T and $M/N\mu_B$ vs. H (inset) for complex **2**.

Magneto-structural comparison

The versatility in coordination modes of oxalate ion in metal complexes (Fig. S6) constitutes the basis for the development of synthesis and magneto-structural investigation of oxalate bridged complexes [here Cu(II) complex] where the magnetic metal centers are as far away as 5 Å. The magnetic coupling in oxalato complexes ranging from weak ferromagnetic (**6-9**)[32,33,35,36] to weak antiferromagnetic (**3-5**)[33,34] through the moderate (**10,11**)[37,38] to strong (**12,13**)[39,40] antiferromagnetic are shown in Table S3 (our synthesized oxalato bridged copper complex is listed as number **2**). Detailed analysis of oxalate bridged Cu(II) complexes establish that their magnetic exchange interactions are strongly dependent on the geometry around the Cu(II) ion, sensitive to the orientation of the magnetic orbital of each Cu(II) ion relative to the oxalate plane and the bridging mode of the oxalate group. It has been found in oxalate-bridged copper(II) complexes that strong antiferromagnetic coupling (J ranging from -260 to -400 cm^{-1}) results when the short Cu(II)–ligand bonds are coplanar with the bridging ligand (topology A in Fig. S7) and the singly occupied molecular orbitals (SOMO's) are built up from metal '*d*' orbitals ($d_{x^2-y^2}$ type orbitals in square pyramidal or elongated octahedral geometry) well oriented to interact with the bridging ligand. When one of the Cu(II)– oxalate bridge distance is long (oxalate bridge is asymmetrically coordinated) the two metal–centred magnetic orbitals are parallel to each other and perpendicular to the bridging oxalate (topology B in Fig. S7) and the interaction is poor which results a weak magnetic coupling (J ranging from +3 to -45 cm^{-1}). An intermediate case is that for which one of the magnetic orbitals is coplanar with the oxalate bridge whereas the other one is perpendicular to it (topology C in Fig. S7),[37] as in complex **2**.

Theoretical study

We have divided the theoretical study into two parts. Firstly, we have analyzed the noncovalent interactions energetically focusing our attention to the C–H/π, anion–π and π–π interactions observed in the solid state of compounds **1** and **2**. In addition, we have also examined the antiparallel intermolecular $NO_3\cdots NO_3$ interaction observed in compound **1**. Similar interactions have been recently attracted attention due to their increasing interest in supramolecular chemistry and crystal engineering.[41] Secondly, we have used DFT calculations combined with the broken symmetry approach to gain insight into the qualitative theoretical interpretation on the overall magnetic behavior of the complex.

Noncovalent interactions

We have focused the theoretical study of compound **1** to the supramolecular 1D chain found in its solid state structure that is characterized by the presence of self-complementary anion–π interactions (Fig. 2). First of all, we have computed and analyzed the MEP surface of complex **1** (X-ray asymmetric unit), that is shown in Fig. 7A. It can be observed that the most positive electrostatic potential isovalue is located close to the aromatic hydrogen atoms of the ligand, which that are more acidic than in the free ligand due to the coordination to the Cu^{II} ion. The blue (positive electrostatic potential) contours also include the π-system and, remarkably, the countour corresponding to the isovalue = +30 kcal/mol reaches the region of the N2–C4 bond. The electrostatic potential over the center of the pyridine ring is smaller (+26 kcal/mol). This result is helpful to explain the location of the uncoordinated oxygen atom (O6, see Fig. 7B) of the nitrate in the X-ray geometry that is pointing to the middle of the C–N bond. We have computed the interaction energy of the self-assembled dimer (see Fig. 7B), which is large and negative (ΔE_1 = –22.4 kcal/mol). A detailed analysis of this dimeric unit reveals that the coordinated nitrate ligands are also interacting to each other (see Fig. 7C). That is, the O4 oxygen atom of one complex is located at 3.065(5) Å from the N5 nitrogen atom of the other complex and *vice versa* (the O4···N5 distance is slightly shorter than the sum of van der Waals radii that is 3.07 Å). This interaction is similar to antiparallel CO···CO interactions described in the literature;[42] however, it should emphasized that in complex **1** the antiparallel NO···NO interaction involves two anionic ligands (even though part of the charge is transfer to the metal center). Therefore this interaction can be considered as a *pseudo* antielectrostatic interaction that has been recently described for hydrogen bonds.[43] In order to investigate if this NO···NO interaction is energetically favored we have used a theoretical model (see Fig. 7D) where the aromatic ligands have been eliminated and only the NO···NO interaction is evaluated. As a result the computed interaction energy is ΔE_2 = –9.1 kcal/mol that indicates a favorable contribution of this interaction. It should be mentioned that this is only a rough estimation of the NO···NO interaction energy because the coordination environment of the Cu ion has changed in this reduced model with respect to complex **1**. However, it likely demonstrates (at least qualitatively) that this *pseudo* antielectrostatic interaction is energetically favorable. Moreover, in an effort to evaluate the anion–π interaction, we have used an additional theoretical model where the nitrate counterions have been replaced by nitrite ligands (see Fig. 7E). This model does not have the contribution of the O6···π interaction that can be then estimated by comparing ΔE_1 and ΔE_3. As a result the contribution of the anion–π interaction (O6···π) to the formation of the dimer is $\Delta E_1 - \Delta E_3$ = -9.8 kcal/mol. We have also used the Bader's "atoms-in-molecules" to further characterize and these interactions and the results are discussed in the SI.

In the polymeric complex **2** we have evaluated energetically the noncovalent interactions that are relevant to rationalize the crystal packing described in Figs. 4 and 5. We have used a repeating structural unit of the polymeric chain of compound **2** for the calculations. The theoretical models to analyze the CH/π and π–π interactions are shown in Fig. 8. The interaction energy of the C–H/π self-assembled complex (Fig. 8A) is larger in absolute value (ΔE_4 = –15.0 kcal/mol) than expected for this type of interaction.[45] This is likely due to additional electrostatic forces between the anionic oxalate ligands and the hydrogen atoms of the methyl groups that are separated by ~3.8 Å (see Fig. 8A). We have also computed a theoretical model where only the organic ligands are considered (see Fig. 8B). As a result the interaction energy is reduced to $\Delta E_5 = -6.8$ kcal/mol indicating that each C–H/π interaction contributes in 3.4 kcal/mol. The π–π interaction mode observed for the coordinated pyridine rings in antiparallel. Previous studies[46] have demonstrated that this arrangement is energetically favored over the parallel binding model. The interaction energy of the π–π model dimer is $\Delta E_6 = -6.7$ kcal/mol that is similar to previously reported in coordinated pyridine and pyrimidine rings (see Fig. 8C).[46] We have also examined the distribution of critical points of both dimeric complexes and a good agreement with the energetic analysis is found (see Fig. S9 in ESI for the results).

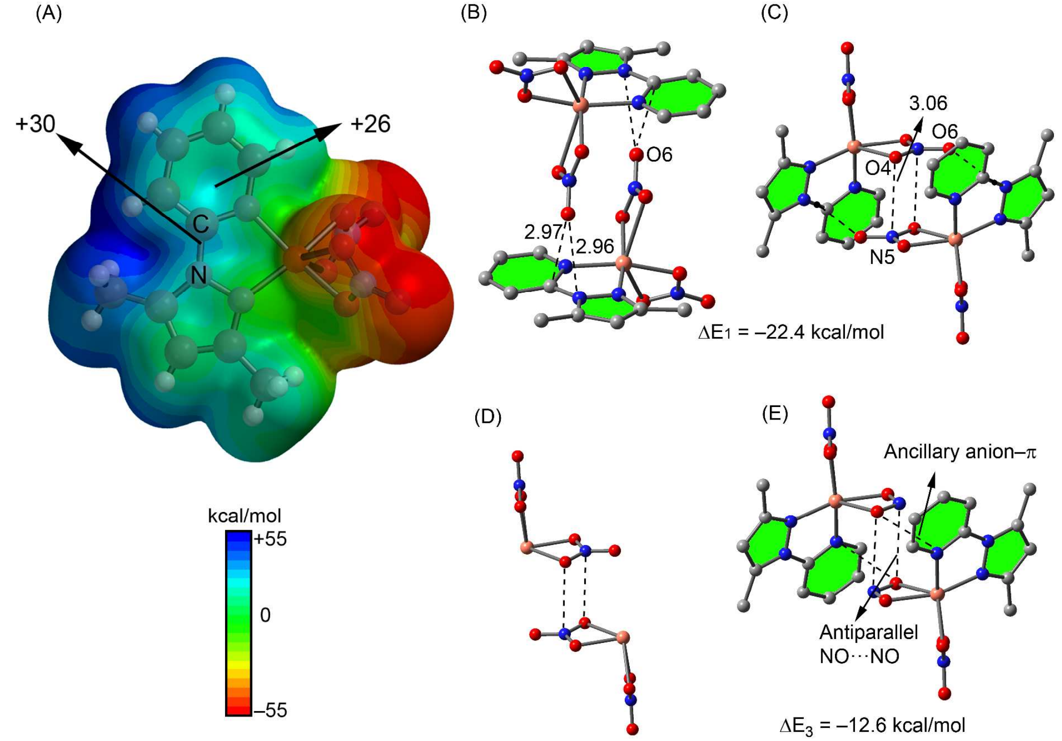

Fig. 7 A) MEP surface computed for **1**. B and C) Two views of the self-assembled dimer observed in the solid state of **1**. (D) Theoretical model without the organic ligands. (E) theoretical model where the nitrate ligands have been replaced by nitrite ligands.

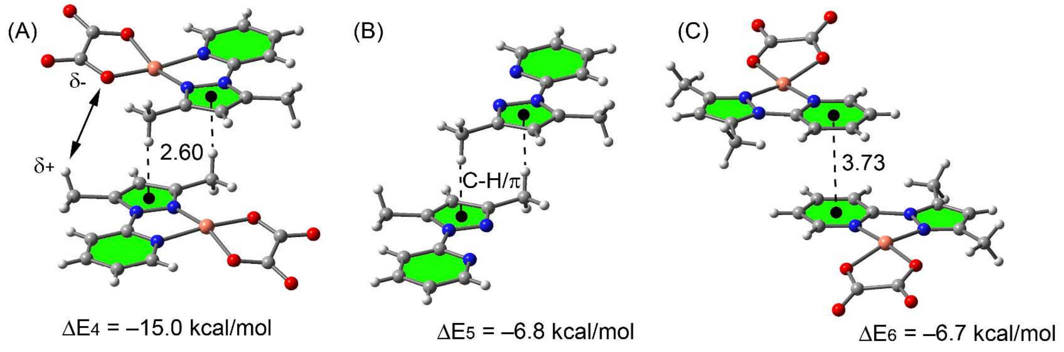

Fig. 8 Theoretical models used to evaluate the noncovalent interactions observed in the solid state of **2** (A-C).

Finally, we have analyzed the the magnetic coupling interaction theoretically in a dinuclear model of compound **2** by computing the spin density distribution. According to the molecular orbital theory, spin delocalization is the result of electron transfer from the magnetic centers to the ligand atoms. A spin-exchange model was generated for theoretical studies using the crystal structure geometry. The theoretical model has been simplified, i.e. hydrogen atoms instead of methyl groups have been used in order to keep the size of the system computationally approachable (Figs. 9A and 9B). The calculation of the individual pair-wise exchange constant has been carried out by means of spin-unrestricted DFT calculations using the B3LYP method and employing the 6-31+G* basis set. The theoretical J value calculation has been performed computing the difference between the energy values of the highest spin state and the broken-symmetry state. Using this methodology and the simplified dinuclear model the theoretical J is 2.4 cm^{-1} that is in good agreement with the experimental value (1.95 cm^{-1}) and confirms the weak ferromagnetic coupling between both metal centers. The Mulliken spin population analysis (Table 4) indicates that a significant spin (ca. 0.73 e) is delocalized through the ligands, and the rest (1.27 e) is carried by the copper atoms. The spin density plot is shown in Fig. 9C for the high spin state of **2**. The spin density distribution shows a delocalization mechanism in which the Cu atoms carry 64 % of net spin and the remaining part is delocalized through coordinating atoms.

Table 4 Mulliken spin densities (e) computed for the high spin configuration of the Cu2 dimer model of compound **2**. See Fig. 9 for numbering scheme

Atom Label	Spin density	Atom Label	Spin density
Cu1	0.62	N1	0.07
Cu1’	0.65	N1’	0.10
O1	0.01	N3	0.05
O2	0.10	N3’	0.06
O3	0.03	C11	-0.00
O4	0.15	C12	-0.01

In a square-pyramidal $\mathrm{Cu^{II}}$ complex, the d_{x2-y2} orbital contains the unpaired electron; consequently these orbitals along with the local orbitals of the bridging ligands are involved in the super-exchange pathway, which is confirmed by the spin density plot shown in Fig. 9C.

The spin density at the O1 is very small (0.01 e) therefore a very weak ferromagnetic coupling is mediated through the bridging ligand communicating the quasi-orthogonal magnetic orbitals. Interestingly, the spin density computed at the carbon atoms of the bridging oxalate group C11 and C12 are negative (-0.003 and −0.010 e, respectively), indicating a spin polarization mechanism that facilitates the ferromagnetic interaction.

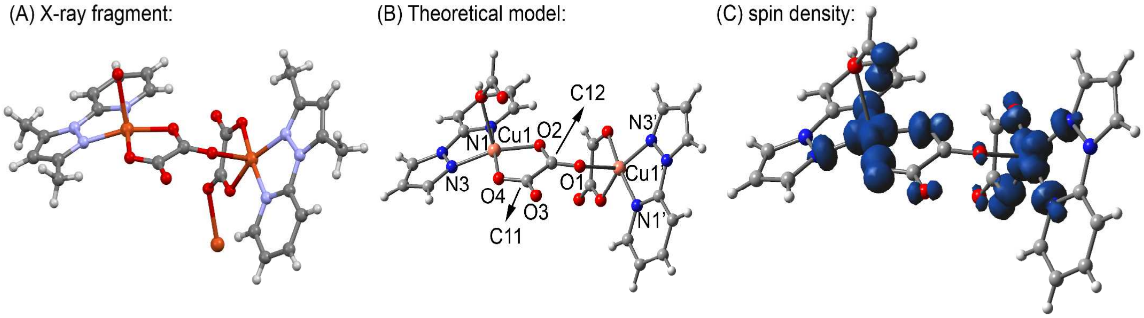

Fig. 9 X-ray, theoretical model and spin density plot (isovalue = 0.004 e $Å^{-3}$) of the dinuclear fragment of complex **2**.

Conclusion

A new one-dimensional oxalate-containing copper(II) complex, namely $[Cu(L)(Ox)_2(H_2O)]_n$ (**2**) has been synthesized by condensing the metal salt with the ligand in methanol solvent and then again by condensing the precursor complex $[Cu(L)(NO_3)_2]$ (**1**) with oxalic acid in aqueous media. The geometry around each Cu(II) in **2** is axially elongated square pyramidal with the intrachain copper-copper separation being 5.399 Å. The magnetic studies reveal a weak ferromagnetic interaction through the oxalate bridge, its nature and magnitude being in a good agreement with available magneto-structural data for oxalate-bridged copper(II) complexes where the same out-of-plane exchange pathway is involved. The DFT calculations combined with the broken symmetry approach provide a good estimate of the weak ferromagnetic coupling that is mediated through the tridentate $\mu_{1,2,3}$ oxalate bridging ligand as corroborated by the spin density plot. Moreover, the interesting noncovalent interactions observed in the solid state have been studied by means of DFT calculations assigning discrete energetic values to them. The most important finding is the *pseudo* antielectrostatic interaction between the nitrato ligands that has been characterized both energetically and using the “atoms-in-molecules” methodology.

Acknowledgements

S. K. acknowledges the financial support provided by University Grants Commission, India (Award letter No. F.4-2/2006(BSR)/13-1089/2013(BSR), dated September, 2013) through the

Dr. D. S. Kothari Post Doctoral Fellowship (DSKPDF). M. S. E. F. acknowledges the financial support from the Spanish Government (Grant CTU2012-30662). Financial support from UGC-UPE (II) program of Jadavpur University is thankfully acknowledged. AF and AB thank the MINECO of Spain for financial support (CONSOLIDER-Ingenio 2010 project CSD2010-0065, FEDER funds) and CTI (UIB) for computational facilities.

References

1 K. Biradha, M. Sarkar and L. Rajput, *Chem. Commun.*, 2006, 4169-4179.

2 N. Hoshino, *Coord. Chem. Rev.*, 1998, **174**, 77-108.

3 M. H. -Molina, P.A. Lorenzo-Luis and C. Ruiz-Pérez, *Cryst. Eng. Comm.*, 2001, **16**, 1-4.

4 S. Youngme, G.A. van Albada, N. Chaichit, P. Gunnasoot, I. Multikainen, O. Roubeau, J. Reedijk and U. Turpeinen, *Inorg. Chim. Acta*, 2003, **353**, 119-128.

5 G. Marinescu, M. Andruh, F. Lloret and M. Julve, *Coord. Chem. Rev.*, 2011, **255**, 161-185.

6 O. Kahn, Molecular Magnetism, Wiley-VCH, New York, 1993, and references therein.

7 H. Núñez, J.-J. Timor, J. Server-Carrió, L. Soto and E. Escrivà, *Inorg. Chim. Acta*, 2001, **318**, 8-14.

8 A. S. Olszewska, B. Matura, J. Mrozinski, B. Kaliuska, R. Kruszynski and M. Penkala, M. *New J. Chem.*, 2014, **38**, 1611-1626.

9 D. Y. Jeter and W. E. Hatfield, *Inorg. Chim. Acta*, 1972, **6**, 523-525.

10 A. Bentana, O. Schott, J. F. Soria, S. E. Stiriba, J. Pasan, C. R. Perez and M. Julve, *Inorg. Chim. Acta*, 2012, **389**, 52-59.

11 U. Geiser, B.L. Ramakrishna, R.D. Wilett, F.B. Hulsbergen and J. Reedijk, *Inorg. Chem.*, 1987, **26**, 3750-3756.

12 A. Gleizes, F. Maury and J. Galy, *Inorg. Chem.*, 1980, **19**, 2074-2078.

13 (a) K. Kadir, T.M. Ahmed, D. Noreus and L. Eriksson, *Acta Crystallogr., Sect. E: Struct. Rep.*, 2006, **62**, 1139-1141; (b) M.-L. Zhu, *Acta Crystallogr., Sect. E: Struct. Rep.*, 2006, **62**, 1985-1987.

14 O. Castillo, A. Luque, F. Lloret, M. Julve and P. Román, *Inorg. Chim. Acta*, 2001, **315**, 9-17.

15 (a) A. Bauzá, T. J. Mooibroek and A. Frontera, *Chem. Commun*., 2015, **51**, 1491-1493; (b) S Roy, A Bauza, A Frontera, R Banik, A Purkayastha, M. G. B. Drew, B. M. Reddy, B. Sridhar, S. Kr. Dasa S. Das, *CrystEngComm*, 2015, **17**, DOI: 10.1039/C5CE00453E.

16 N. Saha and S. K. Kar, *J. Inorg. Nucl. Chem*, 1977, **39**, 1236 – 1238.

17 Bruker, SMART v5.631, Bruker AXS Inc., Madison, WI, USA, 2001.

18 Sheldrick, G.M. SHELXS-97 and SHELXL-97, University of Göttingen, Germany, 1997.

19 (a) L. K. Das, R. M. Kadam, A. Bauzá, A. Frontera and A. Ghosh, *Inorg. Chem*., 2012, **51**, 12407−12418; (b) M. Mitra, P. Manna, A. Bauzá, P. Ballester, S. Kumar Seth, S. R. Choudhury, A. Frontera and S. Mukhopadhyay, *J. Phys. Chem. B*, 2014, **118**, 14713–14726; (c) S. Saha, A. Sasmal, C. R. Choudhury, G. Pilet, A. Bauzá, A. Frontera, S. Chakraborty and S. Mitra, *Inorg. Chim. Acta*, 2015, **425**, 211–220; (d) A. Bauzá and A. Frontera, *Angew. Chem. Int. Ed*., 2015, **54**, 10.1002/anie.201502571.

20 R. Ahlrichs, M. Bär, M. Hacer, H. Horn and C. Kömel, *Chem. Phys. Lett*., 1989, **162**, 165–169.

21 S. Grimme, J. Antony, S. Ehrlich and H. Krieg, *J. Chem. Phys*., 2010, **132**, 154104–19.

22 AIMAll (Version 13.05.06), Todd A. Keith, TK Gristmill Software, Overland Park KS, USA, 2013.

23 (a) A. D. Becke, *Phys. Rev. A*, 1988, **38**, 3098-3100; (b) C. T. Lee, W. T. Yang and R. G. Parr, *Phys. Rev. B*, 1988, **37**, 785-789; (c) A. D. Becke, *J. Chem. Phys*. 1993, **98**, 5648-5653.

24 Gaussian 09, RevisionB.01, M. J. Frisch, G. W. Trucks, H. B. Schlegel, G. E. Scuseria, M. A. Robb, J. R. Cheeseman, G. Scalmani, V. Barone, B. Mennucci, G. A. Petersson, H. Nakatsuji, M. Caricato, X. Li, H. P. Hratchian, A. F. Izmaylov, J. Bloino, G. Zheng, J. L. Sonnenberg, M. Hada, M. Ehara, K. Toyota, R. Fukuda, J. Hasegawa, M. Ishida, T. Nakajima, Y. Honda, O. Kitao, H. Nakai, T. Vreven, J. A. Montgomery, Jr., J. E. Peralta, F. Ogliaro, M. Bearpark, J. J. Heyd, E. Brothers, K. N. Kudin, V. N. Staroverov, R. Kobayashi, J. Normand, K. Raghavachari, A. Rendell, J. C. Burant, S. S. Iyengar, J. Tomasi, M. Cossi, N. Rega, J. M. Millam, M. Klene, J. E. Knox, J. B. Cross, V. Bakken, C. Adamo, J. Jaramillo, R. Gomperts, R. E. Stratmann, O. Yazyev, A. J. Austin, R. Cammi, C. Pomelli, J. W. Ochterski, R. L. Martin, K. Morokuma, V. G. Zakrzewski, G. A. Voth, P. Salvador, J. J. Dannenberg, S. Dapprich, A. D. Daniels, Ö. Farkas, J. B. Foresman, J. V. Ortiz, J. Cioslowski, and D. J. Fox, Gaussian, Inc., Wallingford CT, 2009.

25 (a) E. Ruiz, J. Cano, S. Alvarez and P. Alemany, *J. Comput. Chem*. 1999, **20**, 1391-1400; (b) E. Ruiz, S. Alvarez, A. Rodríguez-Fortea, P. Alemany, Y. Pouillon and C. Massobrio, in: Magnetism: Molecules to Materials (Eds.: J. S. Miller, M. Drillon), Wiley-VCH,Weinheim, Germany, 2001, **2**, 5572; (c) E. Ruiz, A. R. -Fortea, J. Cano, S. Alvarez and P. Alemany, *J. Comput. Chem*. 2003, **24**, 982-989; (d) E. Ruiz, S. Alvarez, J. Cano and V. Polo, *J. Chem. Phys*. 2005, **123**, 164110-164117.

26 P. J. Baesjou, W. L. Driessen, J. Reedjic and A. L. Spek, *Inorg. Chim. Acta*, 2000, **306**, 237-240.

27 C. Adhikari and S. Koner, *Coord. Chem. Rev.* 2010, **254**, 2933-2958.

28 J. H. Aiu, Z. R. Liao, X. J. Meng, L. Zhu, Z. M. Wang and K. B. Yu, *Polyhedron*, 2005, **24**, 1617-1623.

29 L. Y. Wang, B. Zaho, C. X. Zhang, D. Z. Liao, Z. H. Jiang and S. P. Yan, *Inorg. Chem.*, 2003, **43**, 5804-5806.

30 E. Q. Gao, S. Q. Bai, Z. M. Wang and C. H. Yan, *J. Am. Chem. Soc.* 2003, **125**, 4984-4985.

31 F. Murata, M. Arakawa, A. Nakao, K. Satoh and Y. Fukuda, *Polyhedron*, 2007, **26**, 1570-1578.

32 O. Kahn and M. F. Charlot, *Novu. J. Chim.*, 1980, **4**, 567-576.

33 O. Castillo, A. Luque, P. Román, F. Lloret and M. Julve, *Inorg. Chem.*, 2001, **40**, 5526-5535.

34 H. Oshio and U. Nagashima, *Inorg. Chem.*, 1992, **31**, 3295-3301.

35 O. Castillo, A. Luque, F. Lloret and P. Román, *Inorg. Chim. Acta*, 2001, **324**, 141-149.

36 M. L. Calatayud, I. Castro, J. Sletten, F. Lloret and M. Julve, *Inorg. Chim. Acta*, 2000, **300–302**, 846–854.

37 O. Castillo, A. Luque, F. Lloret and P. Roman, *Inorg. Chem. Commun.*, 2001, **4**, 350-353.

38 B. Bag, N. Mondal, S. Mitra, V. Gramlich, J. Ribas and M. S. El. Fallah, *Polyhedron* 2001, **20**, 2113-2116.

39 M. Du, Y. M. Guo and X. H. Bu, *Inorg. Chim. Acta*, 2002, **335**, 136-140.

40 S. Youngme, G. A. V. Albada, N. Chaichit, P. Gunnasoot, P. Kongsaeree, I. Mutikainen, O. Roubeau , J. Reedijk and U. Turpeinen, *Inorg. Chim. Acta*, 2003, **353**, 119-128.

41 (a) A. Bauzá, T. J. Mooibroek and A. Frontera, *Chem. Commun.*, 2015, **51**, 1491-1493; (b) S. Saha, A. Sasmal, G. Pilet, A. Bauzá, A. Frontera and S. Mitra, *CrystEngComm*, 2014, **16**, 654-666.

42 A. Choudhary, D. Gandla, G. R. Krow and R. T. Raines, *J. Am. Chem. Soc.*, 2009, **131**, 7244–7246.

43 F. Weinhold and R. A. Klein, *Angew. Chem. Int. Ed.*, 2014, **53**, 11214-11217.

44 R. F. W. Bader, *Chem. Rev.*, 1991, **91**, 893–928.

45 M. Nishio, *CrystEngComm* 2004, **6**, 130-158.

46 B. K. Mishra, *J. Phys. Chem. A* 2005, **109**, 6-8.

For Table of Contents Use Only

The synthesis of an uncommon oxalate-containing copper(II) chain of formula $[Cu(L)(Ox)_2(H_2O)]_n$ (**2**) and a mononuclear Cu(II) complex $[Cu(L)(NO_3)_2]$ (**1**) are reported. The uncommon π-hole interactions observed in **1** are rationalized using DFT calculations.